Surrogate Modeling Based Multi-objective Dynamic VAR Planning Considering Short-term Voltage Stability and Transient Stability

Tong Han, *Student Member, IEEE,* Yanbo Chen, *Member, IEEE,* Jin Ma, *Member, IEEE,* Yi Zhao, and Yuan-ying Chi

***Abstract*—Transient stability and short-term voltage stability have successively attracted the attention of electric power industry. This paper proposes a novel systematic approach for dynamic VAR planning to improve short-term voltage stability level and transient stability level. The dynamic VAR planning problem is formulated as a multi-objective optimization (MOO) model with objectives including investment cost, short-term voltage stability level and transient stability level. To reduce the complexity of the proposed MOO model, K-means clustering based severe contingencies selection and global sensitivity analysis based potential buses selection are employed, leading to a simplified MOO model. The combination of a surrogate modeling technique called support vector regression and the multi-objective evolutionary algorithm (MOEA) are then used to solve the simplified MOO model, considering both the accuracy of models and the optimization computation cost. This combination makes it feasible to perform multiple runs of MOEAs for weakening the effect of the MOEA's randomness to optimal results and offering more diverse Pareto-optimal solutions for decision makers. Simulations are carried on the IEEE 39-bus system and a real power grid of China, illustrating that our methodology is reliable with high efficiency.**

***Index Terms*—Surrogate modeling, global sensitivity analysis, clustering, multi-objective optimization, reactive power planning, short-term voltage stability, transient stability.**

NOMENCLATURE

x, u, y	Decision variables, state variables and algebraic variables.
$x_{i,m}$	Rated capacity of type m dynamic VAR compensators installed at bus i.
D	Feasible decision space.
$x_{\max,m}$, Δx_m	Maximum rated capacity and minimum capacity interval of type m dynamic VAR compensators.
$C_m(\cdot)$	The cost function of type m dynamic VAR compensators.
$1_{\mathbb{N}_+}(\cdot)$	The indicator function of $\mathbb{N}_+$, and $\mathbb{N}_+$ donates the set of positive integer.
F	Objective functions.
I, I$'$	The set of buses of power systems and initial candidate buses to install dynamic VAR compensators.
I'_p	The set of potential buses to install dynamic VAR compensators.
I'_v, I'_a	The set of potential buses for improving short-term voltage stability level and transient stability level.
M	The set of types of dynamic VAR compensators.
Φ	The set of credible contingencies.
Φ_a, Φ_v	The set of severe contingencies w.r.t. transient stability level and short-term voltage stability level.
Ψ	The set of generators.
T_v, T_a	The time span of short-term voltage stability and transient stability from the contingency cleared.
Γ_v, Γ_a	The set of simulation points in T_v and T_a.
Δt	Time step of time-domain simulation.
$V_{i,t}^k$	Voltage amplitude of bus i at time t after the contingency k.
$V_{i,0}$	Voltage amplitude of bus i at time 0.
$\delta_{i,t}^k$	The rotor angle of generator i at time t after the contingency k.
$\delta_{\mathrm{COI},t}^k$	Center of inertia of system rotor angles at time t after the contingency k.
T_i	Moment of inertia of generator i.
n_b, n_c, n_p	The number of buses in I, I$'$ and I'_p.
n_t	The number of types in M.
n_g	The number of generators in Ψ.
n_s	The number of sample points in global sensitivity analysis.
p_k	The occurrence probability or the weight of contingency k.

This work was supported in part by National Natural Science Foundation of China (51407069) and in part by the Fundamental Research Funds for the Central Universities (2016YQ02)

Tong Han and Yanbo Chen are with the School of Electrical and Electronic Engineering, North China Electric Power University, 102206, Beijing, China (e-mail: hantong.eee@gmail.com; yanbochen2008@sina.com).

Jin Ma is with the School of Electrical and Information Engineering, University of Sydney, NSW, 2006, Australia (e-mail: majinjm@gmail.com).

Yi Zhao is with the School of Electrical Engineering of Southwest Jiaotong University, 611756, Chengdu, China (e-mail: zhaoyi1637@swjtu.edu.cn).

Yuan-ying Chi is with the Future Network Science and Technology Innovation Center, Beijing University of Technology, 100021, Beijing, China (e-mail: goodcyy@126.com).

I. INTRODUCTION

POWER system transient stability and short-term voltage stability have successively attracted the attention of electric power industry. Historically, transient instability has been the dominant stability problem on most transmission systems.

Because of growing use of low inertia compressor motors, air conditioning, voltage-intensive loads and capacitor banks for reactive, as well as more intensive use of transmission, short-term voltage stability of transmission systems has become a greater concern than in the past. Compared with other forms of stability, these two classes of stability are both with period in the order of several seconds and therefore need fast controls to enhance [1], [2].

Dynamic VAR compensators like the static VAR compensator (SVC) and the static synchronous compensator (STATCOM), with suitable controls, can offer fast-acting dynamic reactive power support or damping and hence can efficiently improve short-term voltage stability level and transient stability level, simultaneously or separately [3]. Yet the effectiveness is heavily subject to the size, location, and type of dynamic VAR compensators. Thus the dynamic VAR planning problem has been attracting more and more attention.

The dynamic VAR planning problem was modeled as an optimization problem from power flow point and focused on static voltage stability before, but without considering short-term voltage stability which is the most essential embodiment of the dynamic VAR compensators' profits to voltage stability [4]–[8]. Lately researchers have been solving the dynamic VAR planning problem from dynamic security perspective, taking short-term voltage stability level and transient stability level as constraints or objectives [9]–[14]. From dynamic security perspective, the optimization model of the dynamic VAR planning problem can be divided into two categories: the single-objective dynamic VAR planning model [10]–[13], and the multi-objective dynamic VAR planning model [14]. In [10]–[13], the investment cost of dynamic VAR compensators is modeled as the objective, and short-term voltage stability level and transient stability level are modeled as constraints. By solving the model, the only optimal solution can be got. In [14], the investment cost and short-term voltage stability level are both modeled as objectives. And a set of optimal solutions offering more choices for decision makers can be got by solving the model. Note that the expression of the dynamic process of power systems in the optimization model can greatly affect the selection of optimization algorithms and the practicability of methods. With the dynamic process of power systems expressed explicitly by differential-algebraic equations, classical optimization algorithms are applied with cheap computation cost [10], [11]. In the above approaches, dynamic models of power systems are simplified and only one contingency is considered to make the dimension of variables in optimization acceptable. While with the dynamic process of power systems expressed implicitly by time-domain simulation (TDS) considering accurate models of power systems, derivative-free algorithms like evolutionary algorithms have to be applied [12]–[14]. But this approach is computationally intensive because of expensive function evaluations and the requirement of multiple runs caused by randomness of algorithms. To reduce the complexity of the optimization model, the potential buses are selected before optimizing by numerical approximation-based trajectory sensitivity analysis proposed in [9], a kind of local sensitivity analysis approach [10], [11], [13], [14], or engineering-based analysis [12].

To sum up, there are two shortcomings in the existing dynamic VAR planning approaches: 1) most existing dynamic VAR planning approaches do not take into account the accuracy of power system models and the computation cost of optimization simultaneously [10], [11], [13], [14]; 2) in the exiting dynamic VAR planning approaches, selection of the potential buses, based on the local sensitivity analysis approach or engineering-based approach, does not guarantee to find the correct potential buses in nonlinear power systems sometimes, thus significantly degrading the optimality of the final results [9]–[14].

This paper proposes a novel systematic approach for dynamic VAR planning to improve short-term voltage stability level and transient stability level. The dynamic VAR planning problem is formulated as a multi-objective optimization (MOO) model with objectives including investment cost, short-term voltage stability level and transient stability level. To reduce the complexity of the proposed MOO model, K-means clustering [15] based severe contingencies selection and global sensitivity analysis [16] based potential buses selection are employed, leading to a simplified MOO model. Then the combination of a surrogate modeling technique called support vector regression (SVR) [17] and multi-objective evolutionary algorithms (MOEA) are used to solve the simplified MOO model. The main contributions of this paper are threefold: 1) The proposed approach for dynamic VAR planning considers both the accuracy of power system models and the optimization computation cost. And therefore, it is feasible to perform multiple runs of MOEAs for weakening the effect of the MOEAs randomness on optimal results. 2) The selection of potential buses based on global sensitivity analysis, with robust sensitivity measures even in the presence of nonlinearity, can find the correct potential buses. 3) By modeling both short-term voltage stability level and transient stability level as objectives in the proposed MOO model, more optimal solutions can be obtained for decision makers to make trade-off between investment cost, short-term voltage stability level and transient stability level.

The rest of this paper is organized as follows. The MOO model of the dynamic VAR planning problem is formulated in Section II. Selection of severe contingencies and potential buses are also presented in this section. In Section III, the methodology for solving the MOO model is proposed. Section IV shows the results of proposed dynamic VAR planning approach applied to the IEEE 39-bus system and comparison with existing dynamic VAR planning approaches. Section V offers conclusions.

II. Problem Formulation of Dynamic VAR Planning

In this section, the dynamic VAR planning problem is formulated as an MOO problem making trade-offs between the economic objective and technical objectives. To further reduce the complexity of the MOO model, selection of severe contingencies and potential buses are executed sequentially before optimizing.

A. Basic MOO model for dynamic VAR planning

1) Objectives: The objectives of the dynamic VAR planning problem can be expressed as

$$\min_{x} F = \left[f_1\left(x,u,y\right), f_2\left(x,u,y\right), f_3\left(x,u,y\right) \right] \tag{1}$$

where $x = \left(x_{i,m}\right)^{n_c \times n_t} \in D \subset \left(\mathbb{Z}_0^+\right)^{n_c \times n_t}$ with $i \in \mathrm{I}'$ and $m \in \mathrm{M}$. And $x_{i,m} = 0$ denotes no type m dynamic VAR compensators installed at bus i.

The sub-objective f_1 representing investment cost of dynamic VAR compensators to be installed is calculated as

$$f_1 = \sum_{i \in \mathrm{I}'} \sum_{m \in \mathrm{M}} \left(x_{i,m} C_m(x_{i,m}) \right). \tag{2}$$

where the cost function $C_m(x_{i,m})$ defines the relationship between the cost per unit of type m dynamic VAR compensators and rated capacity of type m dynamic VAR compensators installed at bus i. And $C_m(x_{i,m})$ is a piecewise function expressed as

$$C_m(x_{i,m}) = \begin{cases} c_m^1 & 0 < x_{i,m} \le x_m^1 \\ c_m^2 & x_m^1 < x_{i,m} \le x_m^2 \\ \cdots \end{cases} . \tag{3}$$

where c_m^1 and c_m^2 are constants, and x_m^1 and x_m^2 donates piecewise points [18].

The sub-objective f_2 representing short-term voltage stability level is calculated as

$$f_2 = \sum_{k \in \Phi} \left\{ p_k \left(\sum_{i \in \mathrm{I}} \sum_{t \in \Gamma_v} d_{i,t}^k \right) \Big/ \left(n_b T_v \right) \right\} \tag{4}$$

where

$$d_{i,t}^k = \Delta t \left(\left[\underline{V}_t - V_{i,t}^k \right]^+ + \left[V_{i,t}^k - \overline{V}_t \right]^+ \right). \tag{5}$$

In (5), $[\cdot]^+ = \max(0, \cdot)$. And $\underline{V}_t$ and $\overline{V}_t$ together depict boundaries which the more voltage trajectories overstep, the more short-term voltage stability level is reduced. And they are given by

$$\begin{cases} \underline{V}_t = V_{\mathrm{st}} \left(e^{t/t_{v,\mathrm{end}}} t / t_{v,\mathrm{end}} \right)^{\beta_v} \Big/ e^{\beta_v} \\ \overline{V}_t = 2 - \underline{V}_t \end{cases} \quad \forall t \in \Gamma_v \tag{6}$$

where $t_{v,\mathrm{end}}$ denotes the end instant in Γ_v, β_v is used to calibrate the decaying of the boundaries towards the steady-state value V_{st}.

The sub-objective f_3 representing transient stability level is calculated as

$$f_3 = \sum_{k \in \Phi} \left\{ p_k \left(\sum_{i \in \Psi} \sum_{t \in \Gamma_a} l_{i,t}^k \right) \Big/ \left(n_g T_a \right) \right\} \tag{7}$$

where

$$l_{i,t}^k = \Delta t \left(\left[\underline{\delta}_t - \left(\delta_{i,t}^k - \delta_{\mathrm{COI},t}^k \right) \right]^+ + \left[\delta_{i,t}^k - \delta_{\mathrm{COI},t}^k - \overline{\delta}_t \right]^+ \right) \tag{8}$$

In (8), $\underline{\delta}_t$ and $\overline{\delta}_t$ are with the analogous meaning with $\underline{V}_t$ and $\overline{V}_t$, respectively. And they are given by

$$\begin{cases} \underline{\delta}_t = \delta_{\mathrm{st}} \left(2 - \left(e^{t/t_{a,\mathrm{end}}} t / t_{a,\mathrm{end}} \right)^{\beta_a} \Big/ e^{\beta_a} \right) \\ \overline{\delta}_t = -\underline{\delta}_t \end{cases} \quad \forall t \in \Gamma_a \tag{9}$$

where $t_{a,\mathrm{end}}$ denotes the end instant in Γ_a, β_a is used to calibrate the decaying of the boundaries towards the steady-state value δ_{st}.

The position of COI is calculated as

$$\delta_{\mathrm{COI},t}^k = \left(\sum_{i \in \Phi} \left(T_i \delta_{i,t}^k \right) \right) \Big/ \sum_{i \in \Phi} T_i \ . \tag{10}$$

Here lower values of f_2 and f_3 represent higher short-term voltage stability level and transient stability level, respectively.

In the MOO model, the proposed short-term voltage stability level and transient stability level are both modeled as objectives. Thus more diverse solutions can be obtained and decision makers can be offered more information about POSs to make trade-off between not only the investment cost and short-term voltage stability level but also short-term voltage stability level and transient stability level.

2) Constraints: For power systems, constraints consist of differential-algebraic equation constraints as defined in (11) and pre-disturbance steady state operation constraints. The latter, including voltage amplitude constraints, generators output constraints, etc., can be satisfied by choosing the appropriate operation section.

$$\begin{cases} \dot{u} = h\left(x,u,y\right) \\ 0 = g\left(x,u,y\right) \end{cases} . \tag{11}$$

Without loss of generality, it can be assumed that one certain bus can be installed with at most one type of dynamic VAR compensators. Thus constraints for x are given by

$$\begin{cases} \sum_{m \in \mathrm{M}} 1_{\mathbb{N}_+}\left(x_{i,m}\right) = 1 & \forall i \in \mathrm{I}' \\ 0 \le x_{i,m} \le x_{\max,m} & \forall i, m \in \mathrm{I}', \mathrm{M} \\ x_{i,m} = z \Delta x_m & \forall i, m \in \mathrm{I}', \mathrm{M}; \exists z \in \mathbb{Z}_0^+ \end{cases} . \tag{12}$$

B. Simplified MOO model for dynamic VAR planning

1) Clustering Based Selection of Severe Contingencies: Generally, only severe ones selected from credible contingencies are considered to reduce computing burden [12], [14]. Unlike the manmade selection approach [12], [14], a clustering algorithm, K-means, is used to find severe contingencies. Firstly a brief introduction about K-means is presented.

Let $\boldsymbol{\chi} = \{\chi_i \mid i = 1, \ldots, n\}$ be the set of n d-dimensional points to be clustered into a set of K clusters, $C = \{c_k \mid k = 1, \ldots, K\}$. The K-means algorithm finds a cluster such that the squared error between the empirical mean of a cluster and the points in the cluster is minimized. Let μ_k be the mean of cluster c_k, and the squared error between μ_k and the points in cluster c_k is defined as

$$J\left(c_k\right) = \sum_{\chi_i \in c_k} \left\| \chi_i - \mu_k \right\|^2. \tag{13}$$

And the optimal clustering C^* is given by minimizing the sum of the squared error over all K clusters,

$$C^* = \arg\min_{C} \sum_{k=1}^{K} J\left(c_k\right). \tag{14}$$

Since both short-term voltage stability level and transient stability level are assessed in the MOO model, selection of

severe contingencies is conducted from these two aspects respectively. Yet voltage stability and rotor angle stability are often intertwined [1]. For instability scenarios, the dominant factor between voltage and rotor angle can be distinguished by TDS results including voltage curves and oscillation curves, whereas, for scenarios with drastic voltage drop or severe rotor angle oscillation but without instability, the distinction can be complex. With these in mind, the selection of severe contingencies can be conducted by the following steps.

Step 1): Initialize $\Phi_v = \emptyset$ and $\Phi_a = \emptyset$. $\forall k \in \Phi$, calculate $\chi_k = (f_2 \mid_{\Phi=k,p_k=1}, f_3 \mid_{\Phi=k,p_k=1})$ by TDS.

Step 2): Determine the domain factor for credible contingencies causing instability by TDS results. If a contingency is with continuous drop in bus voltages leading further loss of synchronism of machines, then it is voltage-dominant and add it to Φ_v. And if a contingency is with rapid drop in bus voltages and drastic oscillation due to the loss of synchronism, then it is angle-dominant and add it to Φ_a.

Step 3): Cluster $\boldsymbol{\chi} = \{\chi_k \mid k \in \Phi \wedge k \notin (\Phi_v \cup \Phi_a)\}$ by K-means into a set of 2 clusters, $C = \{c_1, c_2\}$.

Step 4): Suppose c_1 is with more severe contingencies, and thus $\Phi_v = \Phi_v \cup c_1$ and $\Phi_a = \Phi_a \cup c_1$.

Hence, the severe contingencies can be used to assess the short-term voltage stability level and the transient stability level, i.e., Φ is replaced by Φ_v and Φ_a in the calculations of f_2 and f_3, respectively.

2) Global sensitivity analysis Based Selection of Potential Buses: Buses with relatively strong ability to improve the short-term voltage stability level or transient stability level by installing dynamic VAR compensators are called potential buses. For reducing the model complexity so as to shorten optimization time and guarantee the algorithms optimization ability, selecting potential buses as candidate location for potential dynamic VAR compensator installation is a vital step before optimizing. A potential buses selection approach based on global sensitivity analysis is proposed in this subsection. And the global sensitivity measure in [16] is used here.

Only a certain type of dynamic VAR compensators, assumed to be $m' \in \mathrm{M}$ is used in the selection of potential buses. Because the selection of potential buses depends on the sort order of all buses global sensibility measure instead of their values, the choosing of m' generally does not affect the final selection result. After choosing m', in x, $x_{i,m}$ with $i \in \mathrm{I}'$ and $m \in \mathrm{M} \backslash m'$ are fixed at 0, and $x_{i,m}$ with $i \in \mathrm{I}'$ and $m = m'$ are input variables in global sensitivity analysis. And $x_{i,m}$ is shortly denoted as $\widetilde{x}_i$ in the following expression.

Using TDS, we can collect the realization of n_s i.i.d. copies of the pair (X, Y_1, Y_2) in the sample matrix $Z = ((\widetilde{x}_{j,i} \ \ldots \widetilde{x}_{j,n_c} \ y_{j,1} \ y_{j,2})) \in \mathbb{R}^{n_s \times (n_c+2)}$, where $y_{j,1}$ and $y_{j,2}$ correspond to f_2 and f_3 respectively. Considering a fixed bus $i \in \mathrm{I}'$ and the sensitivity w.r.t. short-term voltage stability level, only the n_s-vectors $\widetilde{x}_i = (\widetilde{x}_{j,i})^{n_s \times 1}$ and $y_1 = (y_{j,1})^{n_s \times 1}$ are used in the following discussion. Next we form the scatterplot of $\widetilde{x}_i$ and y_1 and partition the $\widetilde{x}_i$-axis of the scatterplot into V classes, and $V = 5$ is used here. Then the conditional density generated by X_i belonging to this class-interval of a suitably chosen partition $\mathcal{X}_i$ is considered to get any observations conditional to this class. Formally, let $\Lambda = \{C_v \mid v = 1, \ldots, V\}$ with $\bigcup_{v=1}^{V} C_v = \mathcal{X}_i$, $C_v \cap C_{v'} = \emptyset$, $v \neq v'$ denote a partition of $\mathcal{X}_i$ into V classes. The probability of X_i belonging to class C_v is given by

$$P_{X_i}(C_v) = \int_{C_v} f_{X_i}(x)dx. \tag{15}$$

According to the total probability theorem, the class-conditional density of Y_1 given $C_v \subset \mathcal{X}_i$ is given by

$$\begin{aligned} f_{Y_1|C_v}(y_1) &= \frac{\int_{C_v} f_{Y_1|X_i=x}(y_1) f_{X_i}(x)dx}{\int_{C_v} f_{X_i}(x)dx} \\ &= \frac{1}{P_{X_i}(C_v)} \int_{C_v} f_{X_i Y_1}(x, y_1)dx. \end{aligned} \tag{16}$$

Then, we call the quantity

$$S_v = S(C_v) = \int_{y_1} \left| f_{Y_1}(y_1) - f_{Y_1|C_v}(y_1) \right| dy_1 \tag{17}$$

the class separation induced by $C_v \subset \mathcal{X}_i$. Correspondingly, an approximation of the distributional-importance of X_i for partition Λ is defined as

$$\delta_{i,1}^{\Lambda} = \frac{1}{2} \sum_{C \in \Lambda} \left(S(C) P_{X_i}(C) \right) = \frac{1}{2} \sum_{v=1}^{V} \left(S_v P_{X_i}(C_v) \right). \tag{18}$$

By fixing different $i \in \mathrm{I}'$, global sensitivity measures w.r.t. short-term voltage stability level $\delta_1^{\Lambda} = \{\delta_{i,1}^{\Lambda} \mid i \in \mathrm{I}'\}$ and global sensitivity measures w.r.t. transient stability level $\delta_2^{\Lambda} = \{\delta_{i,2}^{\Lambda} \mid i \in \mathrm{I}'\}$ can be got, respectively.

Finally, I'_v and I'_a are defined as (19) and (20) respectively:

$$\mathrm{I}'_v = \mathrm{Top}\left\{ \mathrm{I}' \mid \delta_1^{\Lambda}, n_v, {}'\mathrm{Asc}' \right\}, \tag{19}$$

$$\mathrm{I}'_a = \mathrm{Top}\left\{ \mathrm{I}' \mid \delta_2^{\Lambda}, n_a, {}'\mathrm{Asc}' \right\} \tag{20}$$

where the right-hand side of (19) returns the first n_v buses in I' sorted in δ_1^{Λ} ascending order, and the right-hand side of (20) is analogous. Thus the set of potential buses is:

$$\mathrm{I}'_p = \mathrm{I}'_v \cup \mathrm{I}'_a. \tag{21}$$

And in the MOO model, I' is replaced by I'_p.

Compared with local sensitivity analysis, the global sensitivity analysis allows taking into consideration the entire parameter space so that it provides robust sensitivity measures in the presence of nonlinearity. Thus for nonlinear power systems, global sensitivity analysis based selection of potential buses can find the correct potential buses. It should be noted that the global sensitivity analysis inevitably makes the computation cost heavier, but not unacceptable. For approaches solving the dynamic VAR planning problem by evolutionary algorithms, the total computation cost mainly depends on the optimization process instead of the sensitivity analysis. And expending additional computation cost in selection of potential buses to guarantee optimality of the final solution is worthwhile.

III. Methodology for Solving The Proposed Model

MOEAs enjoy extensive use in coping with MOO models of operation and planning problems in power systems. Yet when solving the MOO model in Section II with MOEAs, massive function evaluations involving expensive TDS are needed. More importantly, because MOEAs search by probabilistic evolutionary operators, final solutions present high variability. A standard practice to avoid this variability is running MOEAs multiply with a distribution of seed for generating random numbers [19]. When MOEAs are applied to solve the proposed MOO model in Section II, despite only the severe contingencies are used to evaluate f_2 and f_3, multiple runs are still infeasible.

Surrogate modeling techniques have been widely used to handle the expensive simulation based function evaluations in optimization. This technique constructs simpler approximation models to predict the system performance. When properly constructed, these approximation models mimic the behavior of the simulation accurately while being computationally cheaper to evaluate.

Motivated by this, we combine a surrogate modeling technique, SVR, and MOEAs to solve the proposed MOO model in this section. The accuracy of models of power systems is assured by TDS, and computation cost is reduced by using surrogate modeling. Therefore, multiple runs for getting high-quality solutions become feasible.

A. Multi-objective Evolutionary Algorithms

1) The Concept of Pareto optimality: In contrast to single-objective optimization, there is typically no single global optimal solution for MOO due to the confliction of objectives. And the optimal solution of MOO is defined by the concept of Pareto optimality, which is defined as follows:

Definition *Pareto Optimal: A solution, $x^* \in D$, is Pareto optimal iff there does not exit another solution, $x \in D$, such that $F(x) \leq F(x^*)$, and $f_i(x) < f_i(x^*)$ for at least one function* [20].

The set of all Pareto optimal solutions (POS) in the space of the decision variables is called the Pareto set (PS); the corresponding values of the objective form the Pareto Front (PF). And the goal of MOEAs is to approximate the PF and get the PS.

2) A Brief Overview of MOEAs: There are large numbers of MOEAs, in which the improved strength Pareto evolutionary algorithm (SPEA2) [21] and the improved nondominated sorting genetic algorithm (NSGA-II) [22] have been widely used in the file of power systems, and the multi-objective evolutionary algorithm based on decomposition (MOEA/D) [23] has been used to cope with the dynamic VAR planning problem. In this paper, these three MOEAs and the reference-point-based many-objective evolutionary algorithm following NSGA-II framework (NSGA-III) [24] are used to prove the randomness of MOEAs and further verify the necessity of multiple runs when solving the dynamic VAR planning problem by MOEAs. NSGA-II, a classical one is used to cope with the proposed MOO model. Here, a brief overview of MOEAs is given, and more introductions to MOEAs and details of the four MOEAs used in our work can be found in [21]–[24] et al.

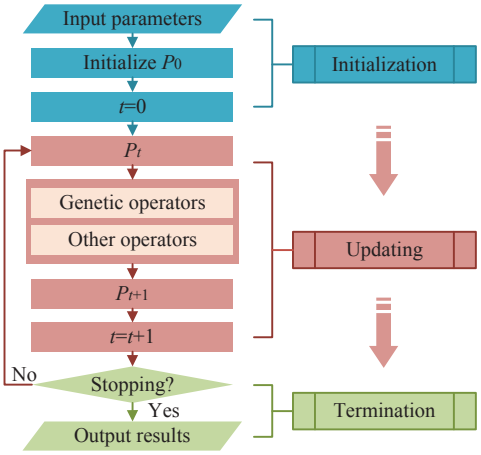

Fig. 1. The general framework of MOEAs.

The general framework of most of MOEAs is shown as Fig. 1. Parameters such as population size and the number of iterations are first set. Except common parameters, the external achieve size and the sub-problem number need to be set for SPEA2 and MOEA/D respectively. Then the initial population P_0 is generated. In each iteration cycle, the current population P_t is updated by genetic operators and other operators varying among different MOEAs.

3) A Convergence Metric of MOEAs: Convergence is usually used to assess the performance of MOEAs. In this paper, we use convergence to prove the need of multiple runs of MOEAs latter. So a convergence metric in [25] is given here.

For the population P_t at t-th generation, the nondominated set D_t is first identified. And then $\forall i \in D_t$, the normalized distance d_i is calculated by:

$$d_i = \max_{j \in P^*} \sqrt{\sum_{k=1}^{M} \left(\frac{f_k(i) - f_k(j)}{f_k^{\max} - f_k^{\min}} \right)^2} \tag{22}$$

where P^* denotes the true PS or a set of reference points which are nondominated. M denotes the number of objectives, and in this paper $M = 3$. $f_k^{\max}$ and $f_k^{\min}$ denote the maximum and the minimum values of k-th function in P^*, respectively. Finally the convergence metric is expressed by averaging the normalized distance for all points in D_t:

$$CM(P_t) = \frac{\sum_{i=1}^{|D_t|} d_i}{|D_t|} \tag{23}$$

B. Surrogate Modeling Based on SVR

In our approach, f_2 and f_3 are evaluated by surrogate models instead of TDS directly in the optimization process. And SVR [17] is used here to build surrogate models.

Suppose the surrogate models of f_2 and f_3 are $\hat{f}_2$ and $\hat{f}_3$ respectively. The first step is generating some points of decision variables based on sampling techniques like space filling sampling or Latin hypercube sampling, and sequentially

collect train data with TDS. Suppose we have got the training data $\Xi = \{(x_1, y_{2,1}, y_{3,1}), \ldots, (x_\ell, y_{2,\ell}, y_{3,\ell})\} \subset \aleph \times \mathbb{R}^2$, where $y_{j,i} = f_j(x_i)$, and $\aleph = \mathbb{R}^{n_p \times n_t}$ denotes the space of input patterns. For brevity, only the calculation of $\hat{f}_2$ is given here, but the analogue is to $\hat{f}_3$. And $y_{2,i}$ is denoted as y_i in the following.

In SVR, x_i is first processed into a higher dimensional feature space $\Im$ by a map $\phi : \aleph \to \Im$. Then the goal is to search a function $f(x)$ with at most ε deviation from the actually obtained targets y_i for all the train data and the highest flatness meanwhile. And thus the function, taking the form

$$f(x) = \langle \omega, \phi(x) \rangle + b \ with \ \omega \in \Im, b \in \mathbb{R} \tag{24}$$

where $\langle \cdot, \cdot \rangle$ is the dot product in $\Im$, is searched. By introducing slack variables ζ_i and ζ_i^* to ensure feasibility, we get the following convex optimization problem:

$$\begin{aligned} \min \ & \frac{1}{2}\langle \omega, \omega \rangle + C \sum_{i=1}^{\ell} (\zeta_i + \zeta_i^*) \\ \text{subject to } & \begin{cases} y_i - \langle \omega, \phi(x_i) \rangle - b \le \varepsilon + \zeta_i \\ \langle \omega, \phi(x_i) \rangle + b - y_i \le \varepsilon + \zeta_i^* \\ \zeta_i, \zeta_i^* \ge 0 \end{cases} \end{aligned} \tag{25}$$

where the constant C reflects the trade-off between the flatness of f and the maximum amount of deviations larger than ε.

Further, applying the method of Lagrange multipliers and saddle point conditions [17], the surrogate of f_2 is given by

$$\hat{f}_2(x) = \sum_{i=1}^{\ell} ((\alpha_i - \alpha_i^*) k(x_i, x)) + b \tag{26}$$

where α_i and α_i^* are Lagrange multipliers. $k(x, x') := \langle \phi(x), \phi(x') \rangle$ is the kernel. Here the kernel of radial basis functions is used:

$$k(x, x') = e^{-\sigma \|x - x'\|^2}, \ \sigma > 0 \tag{27}$$

C. Multi-objective Optimization Based on SVR

To improve the accuracy of surrogate models at the neighborhood of PF, surrogate models are re-build in optimizing by adding training data. The optimization process is as follows.

Step 1): With TDS, generate the initial training data $\Xi = \{(x_1, y_{2,1}, y_{3,1}), \ldots, (x_\ell, y_{2,\ell}, y_{3,\ell})\}$.

Step 2): Calculate the surrogate models $\hat{f}_2$ and $\hat{f}_3$, and then perform the MOEA to get the PS $\{x_1^*, \ldots, x_s^*\}$.

Step 3): Add extra training data to Ξ by the following approach, and repeat Step 2.

Project the PF from the space $f_1 - \hat{f}_2 - \hat{f}_3$ to the plane $\hat{f}_2 - \hat{f}_3$. As shown in Fig. 2, with certain area divided into $n \times n$ grids (in this work, $n = 4$), the Pareto-optimal points nearest to the center of each grid are added to Ξ.

Step 4): If the PS remain the same as the previous one or the maximum number of times $n_{\max}$ that Step 3 has been performed is reached, stop and re-evaluate the PF using f_2 and f_3, and finally output the PS; otherwise go to Step 3.

The flowchart of the proposed dynamic VAR planning approach is shown as Fig. 3. It should be noted that decision making process is also an essential part after obtaining the final PS. Decision makers can determine the final optimal solution with subjective preference, considering restrictions of investment cost as well as requirements of short-term voltage stability level and transient stability level. Moreover, methods for selecting preferred solution from the PS based on fuzzy theory can also be employed [26].

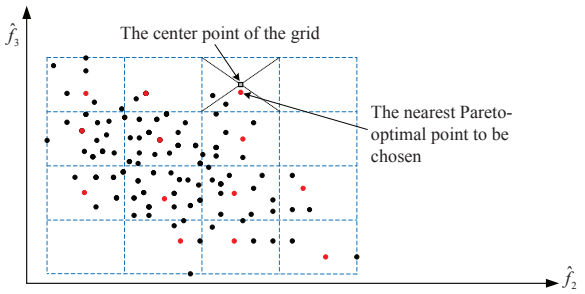

Fig. 2. The schematic of adding points. The minimum rectangular area containing entire Pareto-optimal points is divided into 4×4 grids (the blue dashed grids), and the red Pareto-optimal points nearest to the center of each grid are added to Ξ.

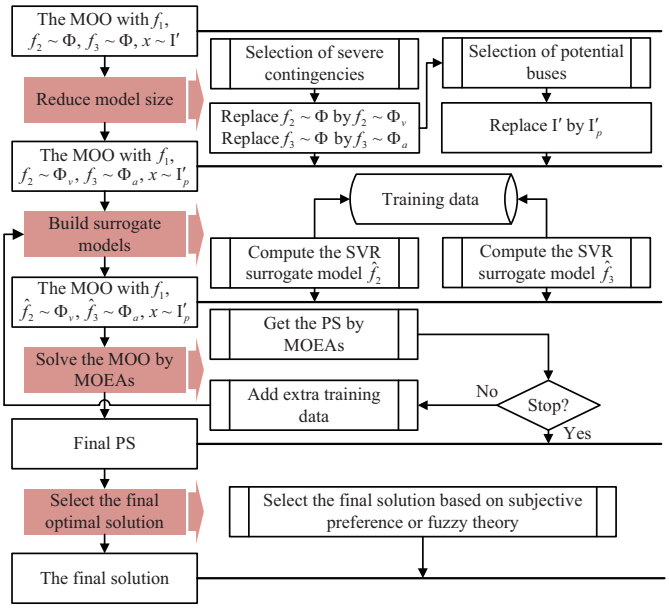

Fig. 3. The flowchart of the proposed dynamic VAR planning approach.

D. Realization of Programs

In this paper, the PSD-BPA (Power System Department - Bonneville Power Administration, a power systems analysis and simulation software) is used to perform the TDS, and all MOEAs used are implemented by the MOEA framework [27], an open source Java framework for MOO. Due to the PSD-BPA offers no interface with programming languages, a PYTHON interface of PSD-BPA is implemented as shown in Fig. 4. A virtual keyboard program in PYTHON, controlling the PSD-BPA like a person controls with the keyboard and the mouse, is developed. A high-performance PYTHON data analysis package, Pandas, is used to process the power system data files imported in the PSD-BPA and the result data files of TDS. Besides, a PYTHON package to allow python programs

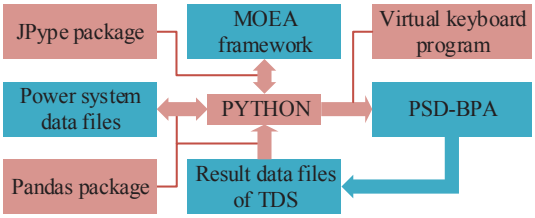

Fig. 4. Realization of Programs

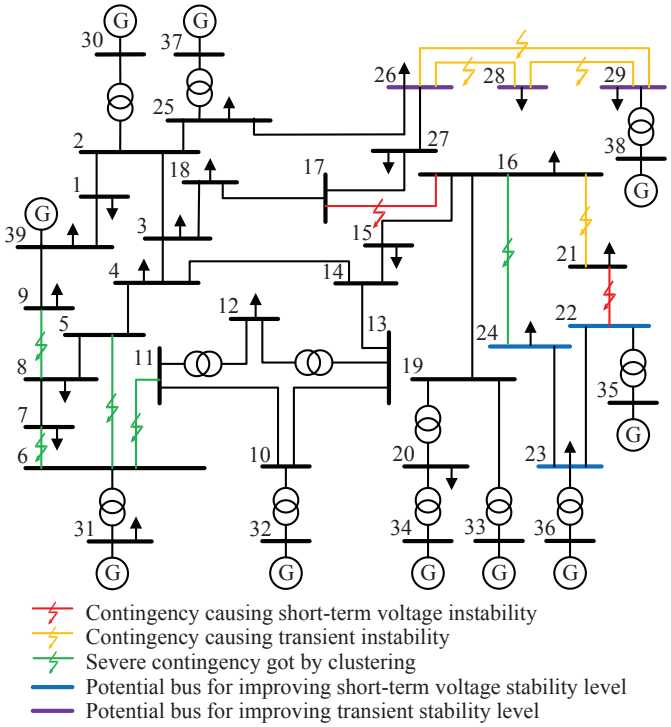

Fig. 5. The diagram of the IEEE 39-bus system.

full access to java class libraries, called JPype, is used to develop the interface between PYTHON and MOEA framework. And other computing is implemented in PYTHON.

IV. Case Study Results

The proposed dynamic VAR planning approach is tested on the IEEE 39-bus system [28]. The diagram of this system is shown in 6. And the merits of the proposed approach are further discussed by comparing with exiting dynamic VAR planning approach. Finally, the application of the proposed approach in a real power grid of China is described.

A. Parameter Settings

The load model can great affect the planning results [14]. In this test, the load model of the IEEE 39-bus system is consisted of 50% small industrial inductor load with parameters taken from [29], 20% constant impedance load, 15% constant current load and 15% constant power load.

Two types of dynamic VAR compensators, SVC and STATCOM, are considered in this test. It is assumed that their maximum rated capacity $x_{\max,m}$ and minimum capacity interval Δx_m are both 400MVar and 10MVar respectively. In practice, $x_{\max,m}$ and Δx_m depend on manufacture level and actual conditions. The cost functions of SVC and STATCOM are shown in Table I [18]. The dynamic models of SVC and STATCOM in [30] are employed and their parameters are obtained from practical engineering.

TABLE I
Cost Functions of SVC and STATCOM

$x_{i,m}$ (MVar)	$C_m(x_{i,m})$ ($ Million/MVar) SVC	STATCOM
$0 < x_{i,m} \leq 100$	0.1	0.13
$100 < x_{i,m} \leq 200$	0.08	0.115
$200 < x_{i,m} \leq 300$	0.07	0.11
$300 < x_{i,m} \leq 400$	0.06	0.1

TABLE II
Results of Selection of Severe Contingencies

Group	FB	χ_k(p.u., °)	Group	FB	χ_k(p.u., °)
1	16-17	$(3.76\times10^{-1}, 1371)$	4	4-14	$(3.78\times10^{-4}, 38.4)$
1	21-22	$(4.55\times10^{-1}, 1962)$	4	5-8	$(8.96\times10^{-4}, 48.0)$
2	16-21	$(2.06\times10^{-2}, 356)$	4	7-8	$(2.01\times10^{-4}, 26.4)$
2	26-28	$(2.04\times10^{-2}, 271)$	4	9-39	$(2.95\times10^{-5}, 21.5)$
2	26-29	$(2.04\times10^{-2}, 315)$	4	10-11	$(3.09\times10^{-4}, 36.9)$
2	28-29	$(1.48\times10^{-2}, 383)$	4	10-13	$(6.53\times10^{-4}, 37.9)$
3	5-6	$(1.96\times10^{-3}, 55.8)$	4	12-11	$(2.63\times10^{-6}, 3.2)$
3	6-7	$(2.00\times10^{-3}, 60.6)$	4	12-13	$(3.04\times10^{-6}, 3.3)$
3	6-11	$(1.99\times10^{-3}, 63.0)$	4	13-14	$(7.34\times10^{-4}, 37.0)$
3	8-9	$(1.57\times10^{-3}, 46.3)$	4	14-15	$(3.35\times10^{-4}, 33.7)$
3	16-24	$(1.43\times10^{-3}, 74.2)$	4	15-16	$(4.88\times10^{-4}, 41.1)$
4	1-2	$(0, 23.7)$	4	17-18	$(4.60\times10^{-3}, 41.1)$
4	1-39	$(2.2\times10^{-6}, 17.0)$	4	17-27	$(4.67\times10^{-4}, 43.5)$
4	2-3	$(3.19\times10^{-4}, 43.6)$	4	22-23	$(1.63\times10^{-4}, 21.9)$
4	2-25	$(2.76\times10^{-4}, 38.8)$	4	23-24	$(1.37\times10^{-4}, 34.3)$
4	3-4	$(3.79\times10^{-4}, 36.4)$	4	25-26	$(1.70\times10^{-4}, 9.1)$
4	3-18	$(3.59\times10^{-4}, 27.1)$	4	26-27	$(2.59\times10^{-4}, 20.3)$
4	4-5	$(4.71\times10^{-4}, 36.8)$			

Notes: FB is the abbreviation of fault branch. $\chi_k = (f_2\,|_{\Phi=k,p_k=1}, f_3\,|_{\Phi=k,p_k=1})$.

Three-phase short circuit faults of branches causing no isolation are taken as credible contingencies. And all faults are assumed to occur in the middle of branches and be cleared after 0.1s by disconnecting the two sides breakers. It is assumed that $\forall k \in \Phi_v$, $p_k = 1/|\Phi_v|$ and $\forall k' \in \Phi_a$, $p_{k'} = 1/|\Phi_a|$.

All non-generator buses in the system are taken as candidate buses to further select potential buses. For real power systems, location of buses and substation physical size should be also taken into account. And STATCOM is used for the sensitivity analysis.

For the calculation of f_2 and f_3, $\beta_v = 0.024$, $V_{\rm st} = 0.9$p.u., $\beta_a = 0.072$ and $\delta_{\rm st} = 60°$ are used [12]. And the time span T_v and T_a are both set to 5 s. For the TDS, the simulation step Δt is set to 0.01s, and the total simulation time for one fault is set to 5.5 s.

B. Selection of Severe Contingencies

Table II shows the results of selection of severe contingencies. The two contingencies in group 1 are with large

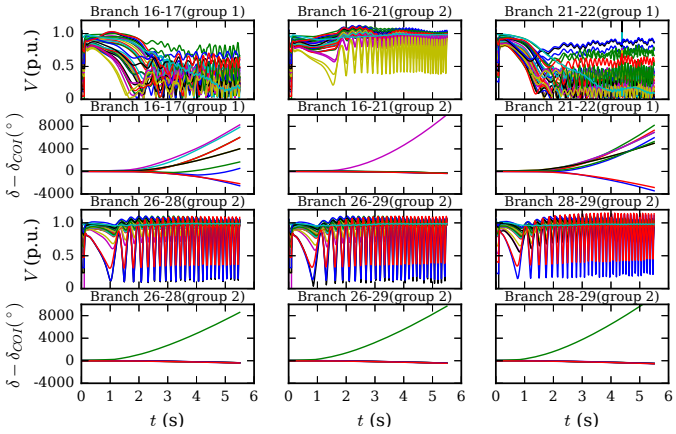

Fig. 6. V-t graphs and $(\delta - \delta_{\mathrm{COI}})$-$t$ graphs of instability contingencies. In the V-t graph, each line represents the voltage curve of one bus. And in the $(\delta - \delta_{\mathrm{COI}})$-$t$ graph, each line represents the oscillation curve of one generator.

values of $f_2\ |_{\Phi=k,p_k=1}$ and $f_3\ |_{\Phi=k,p_k=1}$, that is, they are with quite low short-term voltage stability level and low transient stability level. By post-disturbance voltage curves and oscillation curves in Fig. 6, bus voltages continuously drop in contingencies in group 1, leading further loss of synchronism of machines. Thus voltages are the dominant factor for contingencies in group 1 and they are short-term voltage instability ones. The four contingencies in group 2 are with medium values of $f_2\ |_{\Phi=k,p_k=1}$ and $f_3\ |_{\Phi=k,p_k=1}$. From Fig. 6, in these contingencies the loss of synchronism of two groups of machines causes rapid drop and oscillation in voltages. And contingencies in group 2 are transient instability ones because rotor angles are the dominant factor in these case. Besides, other contingencies are with small values of $f_2\ |_{\Phi=k,p_k=1}$ and $f_3\ |_{\Phi=k,p_k=1}$, causing no obvious instability. By K-means, these contingencies are clustered into two clusters: group 3 with severe contingencies and group 4 with ignored contingencies.

Finally, Φ_v consists of the seven contingencies in group 1 and group 3, and Φ_a consists of the nine contingencies in group 2 and group 3. In the latter calculation, $\forall k \in \Phi_v$, $p_k = 1/7$ and $\forall k' \in \Phi_a$, $p_{k'} = 1/9$.

C. Selection of Potential Buses

To select the potential buses, the global sensitivity presented in Section II-B are evaluated. The results are shown in Fig. 7.

According to Fig. 7, values of the global sensitivity w.r.t. short-term voltage stability level or transient stability level vary among different buses, implying that buses have different ability to improve the short-term voltage stability level or transient stability level by installing dynamic VAR compensators. Moreover, the permutation of buses by the global sensitivity w.r.t. short-term voltage stability level is different from that by the global sensitivity w.r.t. transient stability level, implying that a bus with strong ability to improve the short-term voltage stability level for a dynamic VAR compensator connection may have little effect to improve transient stability. In this test, with $n_v, n_a = 3$, we get $\mathrm{I}'_v = \{22, 23, 24\}$ (blue buses in Fig. 5), $\mathrm{I}'_a = \{26, 28, 29\}$ (purple buses in Fig. 5) and $\mathrm{I}'_p = \{22, 23, 24, 26, 28, 29\}$.

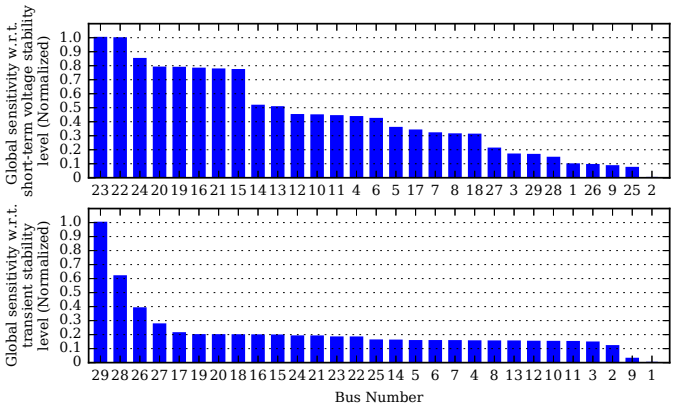

Fig. 7. Global sensitivity of buses w.r.t. short-term voltage stability level (top) and w.r.t. transient stability level (bottom).

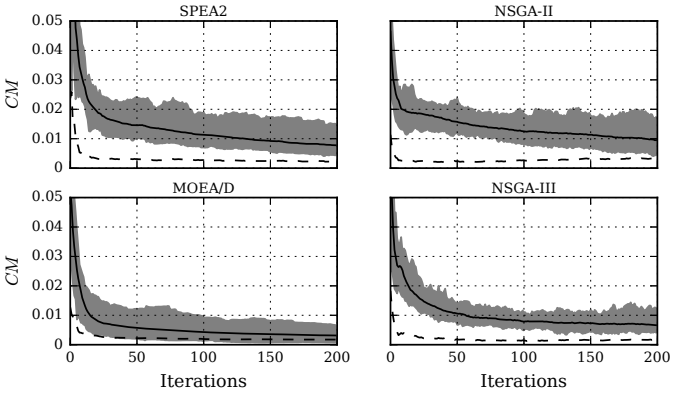

Fig. 8. Dynamic plots of CM versus iterations for SPEA2, NSGA-II, MOEA/D and NSGA-III for 50 random seed trial runs. The range of CM is indicated by the shaded region, the mean by a solid line, and the standard deviation by a dashes line.

D. Necessity of Multiple Runs of MOEAs

To compute the surrogate models, training data with 12225 samples is first generated using space filling sampling combined with Latin hypercube sampling. When training the SVR with kernel of radial basis functions, two parameters must be considered: C and σ. By the grid search and 10-fold cross-validation, $C = 1000$ and $\sigma = 0.1$ are set for $\hat{f}_2$, and $C = 10$ and $\sigma = 0.1$ are set for $\hat{f}_3$.

And then four MOEAs, including SPEA2, NSGA-II, MOEA/D and NSGA-III are used to solve the MOO model, but without adding extra training data. The population size and the number of iterations are both set to 200 for each MOEA. The external achieve size in SPEA2 is set to 200. The number of sub-problems in MOEA/D is set to 20. And 50 random seed trial runs are executed for each MOEA by choosing 50 random seeds. Besides, the PF got by entire runs of each MOEA is used as the P^* for computing whose CM.

Runtime results of CM versus iterations for the four MOEAs are represented in Fig. 8 and randomness of each MOEA is shown. The randomness of SPEA2 and NSGA-II

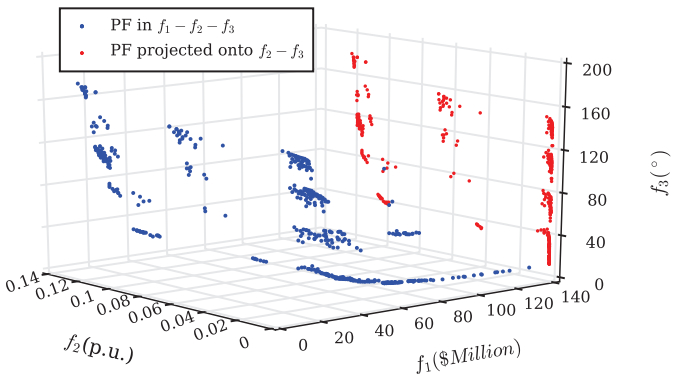

Fig. 9. The PF with 465 solutions after 50 random seed trial runs using NSGA-II. Each blue point or red point corresponds to a POS.

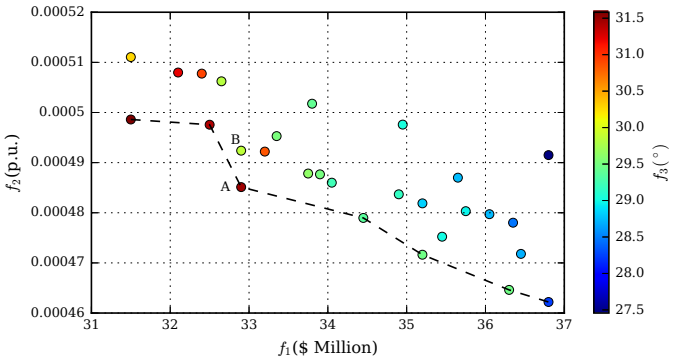

Fig. 10. Partial POSs in the bottom-right of the plane of $f_2 - f_3$ in Fig. 9, with contingencies causing neither short-term voltage instability nor transient instability.

is strong shown by their large shaded region and high values of the standard deviation. For MOEA/D and NSGA-III, the randomness is comparatively week but existent. The end-of-run lower bounds of the shaded region are not equal to 0 for all MOEAs, indicating that it is unreachable to get a subset of the real PF by merely one run. Hence randomness of MOEAs necessitates multiple runs when solving the MOO model of the dynamic VAR planning problem by MOEAs.

E. Final Results

The NSGA-II is used to solve the MOO model, with adding extra training data. The parameter $n_{\max}$ is set to 5. The surrogate models got in Section IV-B are used as the initial surrogate models, and C and σ remain unchanged when re-building the surrogated models. The parameters of NSGA-II are the same as used in Section IV-B. By 50 random seed trial runs, the PF with a total of 465 solutions is obtained as shown in Fig. 9.

From Fig. 9, it can be seen that the PF shows an aggregation trait in the plane of $f_2 - f_3$. Each cluster are with different number of contingencies causing short-term voltage instability or transient instability. Decision maker often are more attentive to the POSs in the bottom-right of the plane of $f_2 - f_3$ in Fig. 9, with contingencies causing neither short-term voltage instability nor transient instability. For clarify, some of POSs from this part are projected onto the $f_1 - f_2$ plane as shown in Fig. 10 for further discussions.

Decision makers can choose the final solution from this part of the PS, according to restrictions of investment cost, and requirements or preferences of short-term voltage stability level and transient stability level. For example, a decision maker claims that investment cost must be strictly less than \$33 million, short-term voltage stability level and transient stability level should be maximum, and transient stability is preferable provided that f_2 is smaller than 0.0005, then the solution B is the final solution.

The details of the solution B is shown in Table III. And after dynamic VAR compensators installation, post-disturbance voltage curves and oscillation curves of contingencies in Fig. 6 which cause short-term voltage instability or transient instability before installation are shown in Fig. 11. It can be

TABLE III
THE FINAL SOLUTION

Type of dynamic VAR compensators	Rated capacity (MVar)					
	Bus 22	Bus 23	Bus 24	Bus 26	Bus 28	Bus 29
SVC	0	0	230	0	30	0
STATCOM	0	0	0	0	0	120

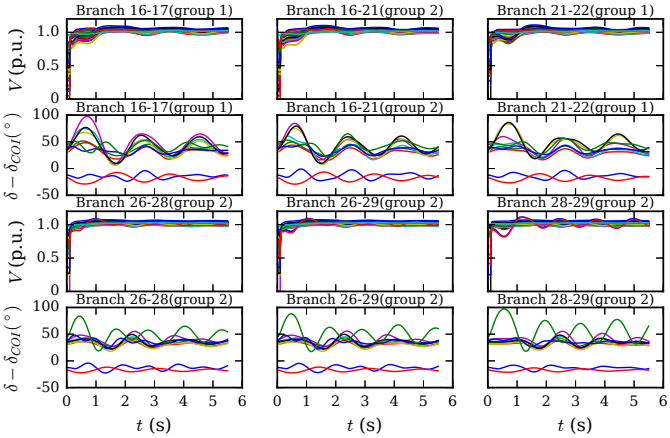

Fig. 11. V-t graphs and $(\delta - \delta_{\mathrm{COI}})$-$t$ graphs of contingencies in Fig. 6 after dynamic VAR compensators installation. The meaning of each line is similar to that of Fig. 6.

seen that with dynamic VAR compensators installation, short-term voltage stability level and transient stability level are both significantly improved, and the system can remain short-term voltage stability as well as transient stability after these contingencies.

F. Comparison with Existing Dynamic VAR Planning Approaches

To further demonstrate the superior performance of the proposed dynamic VAR planning approach, the comparison with three typical dynamic VAR planning approaches proposed in [11], [12], [14] are addressed. The overview of these three approaches can be found in Section I. And Table IV shows the comparison results.

Compared with the approach proposed in [11] which has to employ simply dynamic models of power systems and

TABLE IV
COMPARISON OF EXISTING DYNAMIC VAR PLANNING APPROACHES.

Approach	Accuracy of dynamic models	Computation cost	Contingency considered	Choice space	Optimality
Our approach	High	Average	High	High	High
[11]	Low	High	Low	Low	Low
[12]	High	Average	High	Low	Low
[14]	High	Low	High	Average	Low

Notes: The terms of high, average and low refer to the level of performance in corresponding aspects.

can considerate only one contingency, approach proposed in this paper, [12] and [14] are capable of employing accurate dynamic models of power systems and considering multiple contingencies. These characteristics make these three approach can cope with dynamic VAR planning problem for complex real power systems.

For approaches proposed in this paper and [14], the computation cost mainly consist of that expends in TDS. Assuming that the computation cost of simulating all the severe contingencies once is t_s, the computation cost of the approach proposed in this paper is around $12225 \times t_s$. For obtaining satisfying PS, the approach proposed in [14] also needs multiple runs due to the randomness of MOEAs demonstrated in Section IV-D. Assume that 10 random seed trial runs, which are relatively small in fact, are executed, and the population size and the number of iterations of the MOEA are both 100. Then the computation cost of the approach proposed in [14] is around $1 \times 10^5 \times t_s$. It much exceeds that of the approach proposed in this paper.

As for the choice space for decision makers, approaches proposed in [11] and [12] provide decision makers with only one solution which is a point in Fig. 9, and the approach proposed in [14] provides decision makers with a set of solutions which forms a line in Fig. 9. The approach proposed in this paper, however, can provide the most sufficient optimal solutions which form a surface in Fig. 9 and contain the solutions obtained by approaches proposed in [11], [12] and [14]. Thus decision makes can make trade-off between investment cost, short-term voltage stability level and transient stability level.

When transient stability level is modeled as a constraint and assume that the entire solutions in Fig. 10 satisfy this constraint, solutions on the black dash line form the PS obtained by the approach proposed in [14]. In this case, if decision makers have the same requirements and preferences as the decision maker mentioned in Section IV-E, the solution A will be chosen as the final solution. However, the same decision makers choose the solution B as the final solution with the proposed approach in this paper. These two solutions both meet decision makers' requirements for investment cost and short-term voltage stability level. But the solution B is with higher transient stability level, which is preferable for decision makers. Thus the solution B is superior to the solution A in this decision case. And by modeling both short-term voltage stability level and transient stability level as objectives, diverse POSs can be obtained and decision makers can be offered more information about POSs to make trade-off between not only the investment cost and short-term voltage stability level but also short-term voltage stability level and transient stability level. And thus decision makers can obtain a preferable and superior final solution.

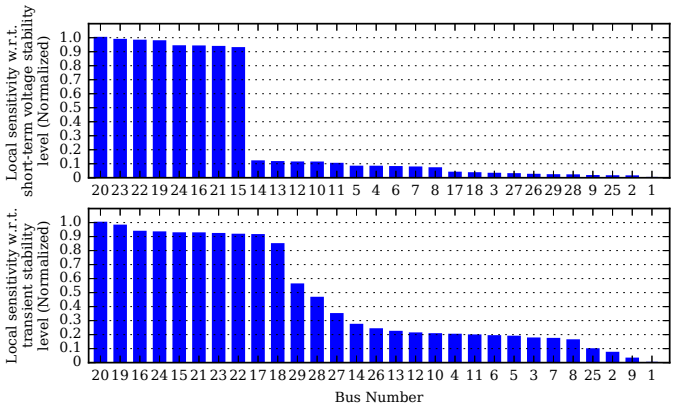

Fig. 12. Local sensitivity of buses w.r.t. short-term voltage stability level (top) and w.r.t. transient stability level (bottom).

The optimality of the final results is greatly affected by correctness of selection of potential buses. The approaches proposed in [11] and [14] select the potential buses base on local sensitivity. To illustrate the limitation of local sensitivity based selection of potential buses, the local sensitivity measure proposed in [14] is computed for all candidate buses with 10Mvar small disturbance. The results are shown in Fig. 12.

From Fig. 7 and 12, it can be seen that permutation of buses by local sensitivity values is different from those by global sensitivity values. When n_v is set to 3, $\mathrm{I}'_v = \{19, 20, 23\}$ by local sensitivity w.r.t. short-term voltage stability level, but which are without the largest global sensitivity values w.r.t. short-term voltage stability level. It is analogue when determining I'_a by local sensitivity w.r.t. transient stability level. So the local sensitivity analysis can find fake potential buses in some cases. A possible method to avoid this failure is to increase n_v and n_a. For example, when n_v is set to 8, I'_v got by local sensitivity is the same as by global sensitivity analysis. Yet in some cases, the increase of n_v and n_a can cripple the effectiveness of selection of potential buses. For example, by the bottom chart in Fig. 7, it is only when n_a is set to larger than 15 that buses of 26, 28 and 29 with the largest global sensitivity values w.r.t. transient stability level can be contained. Thus local sensitivity analysis does not guarantee to find the correct potential buses, thus significantly degrading the optimality of the final results.

To summarize, compared with other three dynamic VAR planning approaches, the approach proposed in this paper considers both the accuracy of dynamic models of power systems and the optimization computation cost. The selection of potential buses based on global sensitivity analysis can find the correct potential buses, ensuring the optimality of the final results. Moreover, the proposed approach can provided decision makers with more optimal solutions to make trade-off between investment cost, short-term voltage stability level and transient stability level.

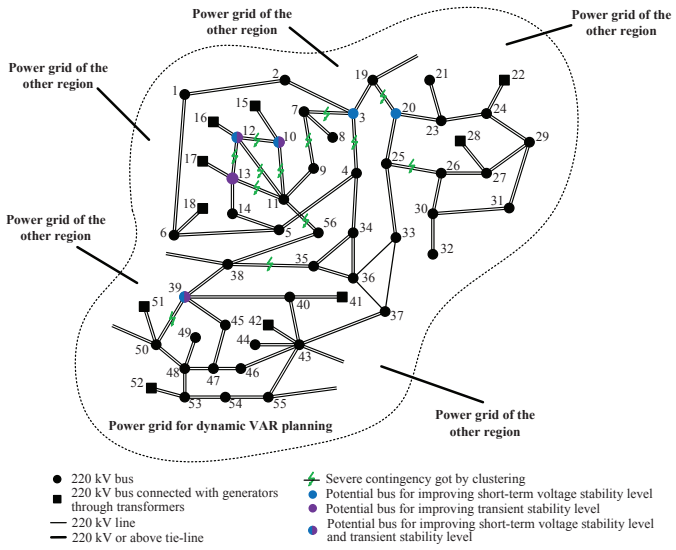

Fig. 13. The power grid for dynamic VAR planning (with only portion of the 220 kV power grid given) and its interconnection with power grids of other regions.

G. Application in the Real Power Grid

The proposed approach is used to cope with the dynamic VAR planning problem of a real 220 kV power grid of China. This grid consists of 205 buses, 215 lines, including 169 double-circuit lines and 46 single-circuit lines, and 29 generating units with a total installed power of about 8150 MW. The forecasting 2020 summer time having a peaking load of 25229.5 MW including 50% dynamic load with almost entirely air conditioner compressor motors is used for the dynamic VAR planning. Due to the critical environmental pollution problems, no more generating units will be installed in this grid in the future, leading to more intensive use of long-distance transmission and potential demand for local dynamic VAR compensation.

From Fig. 13, it can be seen that this power grid is interconnected with power grids of other regions through tie-lines. And for ensuring accuracy, it is not allowed to equate the interconnected power grids in the TDS for dynamic VAR planning. Thus a power grid with a total of 31926 nodes is processed in the TDS. To mitigate the computing burden, the function of parallel batch processing of PSD-BPA is used when performing the TDS.

A total of 215 three-phase short circuit faults of single-circuit lines or one circuit of double-circuit lines with the clearing time of 0.15s are taken as credible contingencies. And 156 220 kV buses with the conditions for installation of dynamic VAR compensators are taken as candidate buses. The load model is derived from load modeling efforts, and p_k and $p_{k'}$ are obtained from historical fault statistics. Other parameters take the same value as in Section IV-A.

After selection of severe contingencies, a total of 13 severe contingencies as shown in Fig. 13 are assigned to Φ_v and Φ_a. All these contingencies are got by clustering and cause neither short-term voltage instability nor transient instability, but relatively serious voltage drop, voltage recovery delay or/and rotor angle oscillation. And then, a total of 6 buses, including 4 buses for improving short-term voltage stability level and 3 buses for improving transient stability level as shown in Fig. 13, are selected as potential buses. Finally, after computing the surrogate models with 12225 training samples and executing 50 random seed trial runs of NSGA-II, a total of 582 POSs are obtained and decision makers can make further trade-off based on their subjective preference.

It should be mentioned that the computing burden of the TDS for selection of severe contingencies, selection of potential buses and especially collecting training samples increases substantially for the large-scale power grid. To mitigate this computing burden, some powerful computing technologies, such as parallel computing mentioned above and distributed computing, can be applied when performing the TDS.

V. Conclusion

In this paper, a novel systematic approach is proposed for dynamic VAR planning. The dynamic VAR planning problem is formulated as an MOO model with objectives including investment cost, short-term voltage stability level and transient stability level. K-means and global sensitivity analysis are first used respectively for selection of severe contingencies and potential buses to reduce the model complexity. And then the reduced MOO model is solved by the combination of SVR and MOEAs. Numerical experiments verify the proposed method. The global sensitivity analysis based potential buses selection approach can find the real potential buses. The proposed approach takes into account both accuracy of models of power systems and optimization computation cost and make multiple runs of MOEAs feasible. By multiple runs, the effect on optimal results from randomness of MOEAs is weakened and decision makers can also get more diverse POSs. By modeling short-term voltage stability level and transient stability level as objectives, decision makers can get more information about solutions and seek more profits on both of them.

A total computation is required for the proposed approach when the power system operation status selected for dynamic VAR planning changes. Thus when considering uncertainties of power system operation status such as load change, topology change and change of percentage of dynamic load, the proposed approach becomes time-consuming. A dynamic VAR planning methodology combining the surrogate modeling technique and robust optimization theory is currently being pursued.

References

[1] P. Kundur, J. Paserba, V. Ajjarapu, G. Andersson, A. Bose, C. Canizares, N. Hatziargyriou, D. Hill, A. Stankovic, C. Taylor, T. V. Cutsem, and V. Vittal, "Definition and classification of power system stability ieee/cigre joint task force on stability terms and definitions," *IEEE Trans. Power Syst.*, vol. 19, no. 3, pp. 1387–1401, Aug 2004.

[2] J. A. D. de Leon and C. W. Taylor, "Understanding and solving short-term voltage stability problems," in *Power Engineering Society Summer Meeting, 2002 IEEE*, vol. 2, July 2002, pp. 745–752 vol.2.

[3] N. G. Hingorani and L. Gyugyi, *Static Shunt Compensators: SVC and STATCOM*. Wiley-IEEE Press, 2000, pp. 135–207. [Online]. Available: http://ieeexplore.ieee.org/xpl/articleDetails.jsp?arnumber=5264273

[4] S. Gerbex, R. Cherkaoui, and A. J. Germond, "Optimal location of multi-type facts devices in a power system by means of genetic algorithms," *IEEE Trans. Power Syst.*, vol. 16, no. 3, pp. 537–544, Aug 2001.

[5] N. Yorino, E. E. El-Araby, H. Sasaki, and S. Harada, "A new formulation for facts allocation for security enhancement against voltage collapse," *IEEE Trans. Power Syst.*, vol. 18, no. 1, pp. 3–10, Feb 2003.
[6] A. Sode-Yome, N. Mithulananthan, and K. Y. Lee, "A maximum loading margin method for static voltage stability in power systems," *IEEE Trans. Power Syst.*, vol. 21, no. 2, pp. 799–808, May 2006.
[7] Y. C. Chang, "Multi-objective optimal svc installation for power system loading margin improvement," *IEEE Trans. Power Syst.*, vol. 27, no. 2, pp. 984–992, May 2012.
[8] E. Ghahremani and I. Kamwa, "Optimal placement of multiple-type facts devices to maximize power system loadability using a generic graphical user interface," *IEEE Trans. Power Syst.*, vol. 28, no. 2, pp. 764–778, May 2013.
[9] B. Sapkota and V. Vittal, "Dynamic var planning in a large power system using trajectory sensitivities," *IEEE Trans. Power Syst.*, vol. 25, no. 1, pp. 461–469, Feb 2010.
[10] A. Tiwari and V. Ajjarapu, "Optimal allocation of dynamic var support using mixed integer dynamic optimization," *IEEE Trans. Power Syst.*, vol. 26, no. 1, pp. 305–314, Feb 2011.
[11] M. Paramasivam, A. Salloum, V. Ajjarapu, V. Vittal, N. B. Bhatt, and S. Liu, "Dynamic optimization based reactive power planning to mitigate slow voltage recovery and short term voltage instability," *IEEE Trans. Power Syst.*, vol. 28, no. 4, pp. 3865–3873, Nov 2013.
[12] S. Wildenhues, J. L. Rueda, and I. Erlich, "Optimal allocation and sizing of dynamic var sources using heuristic optimization," *IEEE Trans. Power Syst.*, vol. 30, no. 5, pp. 2538–2546, Sept 2015.
[13] W. Huang, K. Sun, J. Qi, and Y. Xu, "Voronoi diagram based optimization of dynamic reactive power sources," in *2015 IEEE Power Energy Society General Meeting*, July 2015, pp. 1–5.
[14] Y. Xu, Z. Y. Dong, K. Meng, W. F. Yao, R. Zhang, and K. P. Wong, "Multi-objective dynamic var planning against short-term voltage instability using a decomposition-based evolutionary algorithm," *IEEE Trans. Power Syst.*, vol. 29, no. 6, pp. 2813–2822, Nov 2014.
[15] C. Bishop, *Pattern Recognition and Machine Learning*. Springer-Verlag, 2006.
[16] E. Plischke, E. Borgonovo, and C. L. Smith, "Global sensitivity measures from given data," *European Journal of Operational Research*, vol. 226, no. 3, pp. 536–550, 2013.
[17] A. J. Smola and B. Schölkopf, "A tutorial on support vector regression," *Statistics and computing*, vol. 14, no. 3, pp. 199–222, 2004.
[18] B. M. Wilamowski and J. D. Irwin, *Power electronics and motor drives*. CRC Press, 2016.
[19] C. C. Coello, G. B. Lamont, and D. A. Van Veldhuizen, *Evolutionary algorithms for solving multi-objective problems*. Springer Science & Business Media, 2007.
[20] K. Miettinen, *Nonlinear multiobjective optimization*. Springer Science & Business Media, 2012, vol. 12.
[21] E. Zitzler, M. Laumanns, L. Thiele *et al.*, "Spea2: Improving the strength pareto evolutionary algorithm," in *Eurogen*, vol. 3242, no. 103, 2001, pp. 95–100.
[22] K. Deb, A. Pratap, S. Agarwal, and T. Meyarivan, "A fast and elitist multiobjective genetic algorithm: Nsga-ii," *IEEE Trans. Evol. Comput.*, vol. 6, no. 2, pp. 182–197, Apr 2002.
[23] Q. Zhang and H. Li, "Moea/d: A multiobjective evolutionary algorithm based on decomposition," *IEEE Trans. Evol. Comput.*, vol. 11, no. 6, pp. 712–731, Dec 2007.
[24] K. Deb and H. Jain, "An evolutionary many-objective optimization algorithm using reference-point-based nondominated sorting approach, part i: Solving problems with box constraints," *IEEE Trans. Evol. Comput.*, vol. 18, no. 4, pp. 577–601, Aug 2014.
[25] V. Khare, X. Yao, and K. Deb, "Performance scaling of multi-objective evolutionary algorithms," in *International Conference on Evolutionary Multi-Criterion Optimization*. Springer, 2003, pp. 376–390.
[26] C. J. Ye and M. X. Huang, "Multi-objective optimal power flow considering transient stability based on parallel nsga-ii," *IEEE Trans. Power Syst.*, vol. 30, no. 2, pp. 857–866, March 2015.
[27] D. Hadka. (2015) Moea framework user guide. version 2.7. [Online]. Available: http://moeaframework.org/
[28] A. Pai, *Energy function analysis for power system stability*. Springer Science & Business Media, 2012.
[29] P. Kundur, *Power system stability and control*. McGraw-hill New York, 1994.
[30] Y. Ying, Y. Tang, and B. Li, *User manual of PSD-BPA stability programs*. China Electric Power Research Institute, 2012.

Tong Han (S'15) received the B.S. degrees in electrical engineering from North China Electric Power University in 2015, where he is currently pursuing the M.S. degree in electrical engineering with the School of Electrical and Electronic Engineering. His research interests include power system optimization and cyber-physical system security.

Yanbo Chen (M'13) received the B.S., the M.S. and the Ph.D. degrees in electrical engineering from Huazhong University of Science and Technology, China Electric Power Research Institute, Tsinghua University, in 2007, 2010 and 2013, respectively. He is currently an associate professor of North China Electric Power University. His research interests include state estimation and power system analysis and control.

Jin Ma (M'06) received the B.S. and M.S. degree in electrical engineering from Zhejiang University, Hangzhou, China, the Ph.D. degree in electrical engineering from Tsinghua University, Beijing, China, in 1997, 2000, and 2004, respectively. He is currently with the School of Electrical and Information Engineering, University of Sydney. His major research interests are load modeling, nonlinear control system, dynamic power system, and power system economics. He is the member of CIGRE W.G. C4.605 Modeling and aggregation of loads in flexible power networks and the corresponding member of CIGRE Joint Workgroup C4-C6/CIRED Modeling and dynamic performance of inverter based generation in power system transmission and distribution studies. He is a registered Chartered Engineer.

Yi Zhao received the B.S. degree and the Ph.D. degree in electrical engineering from Southwest Jiaotong University and Tsinghua University, in 2008 and 2013, respectively. She currently works as a teaching assistant in the School of Electrical Engineering of Southwest Jiaotong University. Her research interests focus on power system analysis and control.

Yuan-ying Chi received her B.S. in Northeast Electric Power University, the M.S. and Ph.D. in Jilin University of China. She is currently a professor in Future Network Science and Technology Innovation Center, Beijing University of Technology. Her major research interests are low carbon economy and new energy, energy industry economy, carbon trading and carbon financial research.